

Microscopic Dynamics of Recovery in Sheared Depletion Gels

B. Chung,¹ S. Ramakrishnan,² R. Bandyopadhyay,³ D. Liang,³ C. F. Zukoski,⁴ J. L. Harden,^{1,5,*} and R. L. Leheny^{3,†}

¹*Department of Chemical and Biomolecular Engineering, Johns Hopkins University, Baltimore, Maryland 21218, USA*

²*Department of Chemical and Biomedical Engineering, Florida State University and Florida A&M University, Tallahassee, Florida 32310, USA*

³*Department of Physics and Astronomy, Johns Hopkins University, Baltimore, Maryland 21218, USA*

⁴*Department of Chemical and Biomolecular Engineering, University of Illinois, Urbana, Illinois 61801, USA*

⁵*Department of Physics, University of Ottawa, Ottawa, Ontario K1N 6N5, Canada*

(Received 11 December 2005; published 6 June 2006)

We report x-ray photon correlation spectroscopy and diffusing wave spectroscopy studies of depletion gels formed from nanoscale silica colloids in solutions of nonabsorbing polymer following the cessation of shear. The two techniques provide a quantitatively coherent picture of the dynamics as ballistic or convective motion of colloidal clusters whose internal motion is arrested. While the dynamics possesses features characteristic of nonergodic soft solids, including a relaxation time that grows linearly with the time since shear, comparison with behavior of quenched supercooled liquids indicates that this evolution is not directly related to traditional aging phenomena in glasses.

DOI: [10.1103/PhysRevLett.96.228301](https://doi.org/10.1103/PhysRevLett.96.228301)

PACS numbers: 82.70.Gg, 62.25.+g, 64.70.Pf, 82.70.Dd

For a wide assortment of disordered soft solids—such as foams, gels, concentrated emulsions, and dense colloidal suspensions—the solid phase is separated from a fluid state by an ergodic-nonergodic transition that leaves the system in an out-of-equilibrium configuration. For dense colloids, mode coupling theory provides a framework for this transition, and recently the theory has been extended to colloids with attractive interactions undergoing structural arrest [1–3]. Another approach for understanding such ergodic-nonergodic transitions is the concept of jamming [4,5], which has been invoked to unify a range of fluid-solid transitions in disordered soft matter and to connect them to the glass transition in supercooled liquids. As part of the jamming phase diagram, nonergodic solids can be made fluid by sufficiently large shear stress. A central feature of liquids quenched through the glass transition is the subsequent evolution of their dynamic and thermodynamic properties, a process known as aging [6,7]. An important question, therefore, is whether other routes through ergodic-nonergodic transitions, for example, changes in shear stress, lead to nonergodic states that evolve in the same way. Similarities observed between the behavior of disordered soft solids following cessation of shear and aging in glasses [8–10] as well as theoretical treatments [11–16] lend credence to such a connection; however, other recent theory has questioned this connection [17].

In this Letter, we investigate the nature of recovery from shear in jammed suspensions of concentrated, attractive nanoparticles from a microscopic perspective by combining two complementary techniques, x-ray photon correlation spectroscopy (XPCS) and diffusing wave spectroscopy (DWS), that are uniquely suited for characterizing nanoscale motions over a broad range of time scales. The nanoparticles experience an entropic depletion attraction due to the presence of a nonabsorbing polymer [18]. The suspensions, consisting of octadecyl-grafted silica colloids

(radius, $R \approx 45$ nm) in decalin with added polystyrene (radius of gyration, $R_g \approx 3.5$ nm), display an ergodic-nonergodic transition as a function of colloid volume fraction and strength of attraction, as tuned via polymer concentration. This phase behavior and corresponding structure and mechanical properties are well characterized [19–21], allowing us to focus on the evolution of the microscopic dynamics following shear. We find this dynamics is described by ballistic motion of micron-scale particle clusters in response to stress, with the internal structure of the clusters remaining arrested.

The experiments were performed on suspensions with colloidal volume fractions $0.25 < \phi < 0.36$ and polymer concentrations $0.14 < c_p/c_p^* < 0.3$, where $c_p^* = 0.16$ g/ml is the polymer overlap concentration. Over this range of ϕ and c_p/c_p^* , the suspensions are in the nonergodic gel state. Fluidization of these quiescent solids was accomplished by extrusion through a needle of length 38 mm and inner diameter 0.255 mm at a controlled rate of 0.67 ml/min, corresponding to an average shear rate of approximately 4300 s^{-1} [22]. The recovery time t_d was measured from the cessation of shear.

For the XPCS experiments, suspensions were extruded into sealable, stainless-steel sample holders with thin polyimide windows for transmission scattering and sample thickness 0.5 mm. The experiments were performed at sector 8-ID of the Advanced Photon Source (APS) using 7.66 keV x rays. Details regarding the beam line have been presented elsewhere [23]. The temperature of the samples was held at 25 °C throughout the measurements. The scattering intensity was recorded by a direct-illuminated CCD area detector 3.4 m after the sample to cover a wave-vector range $0.04 < q < 0.39 \text{ nm}^{-1}$. At different t_d , a series of scattering images was recorded to determine the ensemble-averaged intensity autocorrelation function $g_2(q, t)$ [23]. Each measurement of $g_2(q, t)$ was performed on a fresh

region of the sample to avoid radiation damage. The minimum delay time t was 2.6 s. The longest delay time was limited to 1000 s to avoid artificial decays in $g_2(q, t)$ at larger t due to instrumental effects. The intermediate scattering function $g_1(q, t)$ was calculated from $g_2(q, t)$ using the relation, $g_2(q, t) = 1 + Ag_1^2(q, t)$, where A is the Siegert factor that depends on instrumental conditions [23]. Measurements on static aerogel samples determined $A \approx 0.22$, consistent with a value expected based on the x-ray optics.

Figure 1 displays the intermediate scattering function $g_1(q, t)$ determined with XPCS at $q = 0.09 \text{ nm}^{-1}$ on a suspension with $\phi = 0.33$ and $c_p/c_p^* = 0.18$ (gel A) at several recovery times t_d . The inset in Fig. 1 shows the scattering intensity $I(q)$ measured at the same t_d , revealing the interparticle structure factor peak near $q = 0.16 \text{ nm}^{-1}$ and low q intensity due to longer-range correlations [20]. The measured $I(q)$ are unnormalized; therefore, we normalize the curves so that the interparticle peak heights match. As Fig. 1 illustrates, the microscopic dynamics evolve rapidly as the system recovers from the shear. To prevent this rapid evolution from distorting the measured line shape, we restrict analysis of $g_1(q, t)$ to $t < t_d/10$, so that each $g_1(q, t)$ is a “snapshot” of the dynamics at a given t_d . As the inset illustrates, these rapidly evolving dynamics are accompanied by essentially no change in the shape of $I(q)$. This insensitivity of structure to the dynamical recovery from shear is reminiscent of the behavior of glasses, which display few if any structural signatures of aging.

Measurements on other suspensions over the experimental range of ϕ and c_p/c_p^* revealed dynamics very similar to those in Fig. 1. We therefore focus on two suspensions, one with $\phi = 0.33$ and $c_p/c_p^* = 0.18$ (gel A) and one with $\phi = 0.28$ and $c_p/c_p^* = 0.20$ (gel B), for which we obtained the most complete sets of XPCS results. To model their dynamical behavior, we fit the results for $g_1(q, t)$ to

the form $g_1(q, t) = \exp[-(t/\tau)^\beta]$. The solid lines in Fig. 1 show the results of such fits, which describe accurately $g_1(q, t)$ at all q and at all t_d . The characteristic relaxation time τ extracted from the fits, shown in Fig. 2(a) for the two suspensions at $q = 0.09 \text{ nm}^{-1}$, scales roughly linearly with t_d . Such scaling has been identified in a wide range of materials as a signature feature of aging. The exponent β extracted from the fits has a value $\beta = 1.48 \pm 0.12$ independent of q and t_d . $\beta > 1$ implies that the correlation function has a “compressed” exponential line shape. Figure 2(b) displays τ as a function of q at $t_d = 3200$ s for the two suspensions. The dashed line in Fig. 2(b) shows the relation $\tau \sim q^{-1}$, which accurately describes the wave-vector dependence at all t_d .

Such compressed exponential correlation functions with $\tau \sim q^{-1}$ are inconsistent with diffusive dynamics. Instead, as discussed by Cipelletti *et al.* [24], they indicate ballistic motion with a broad distribution of velocities and a characteristic velocity of $V_0 = 1/(\tau q)$. The linear increase in τ with t_d thus implies $V_0 \sim t_d^{-1}$. Essentially identical line shape and wave-vector dependence have been observed in a number of jammed soft solids including colloidal gels [25], clay suspensions [26,27], and concentrated emulsions [24]. Cipelletti *et al.* [24] have advanced a microscopic picture for these ballistic dynamics, describing them in terms of elastic strain deformation in response to heterogeneous local stress. Modeling the source of this stress as local rearrangements of particles that create dipolar stress fields, Bouchaud and Pitard [28] have shown how the resulting strain leads to a compressed exponential line shape and $\tau \sim q^{-1}$. Thus, we interpret the particle-scale dynamics associated with the recovery from shear of the suspensions with this same class of dynamics.

To understand better the ballistic dynamics, we have conducted DWS experiments [29,30] on the same suspensions as in the XPCS study, subjecting them to the same shear history. The DWS was performed using a combined

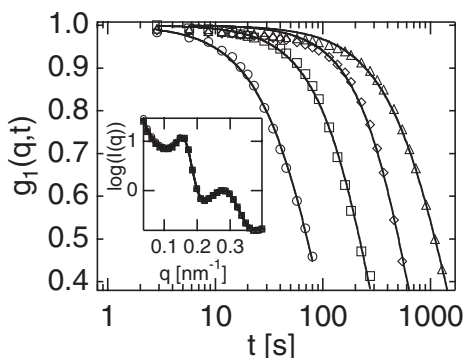


FIG. 1. XPCS intermediate scattering functions at $q = 0.09 \text{ nm}^{-1}$ for gel A following the application of strong shear for recovery times $t_d = 800$ (circles), 2500 (boxes), 6100 (diamonds), and 13 000 s (triangles). The solid lines are the results of fits to a compressed exponential form. The inset shows the x-ray scattering intensity for these different times.

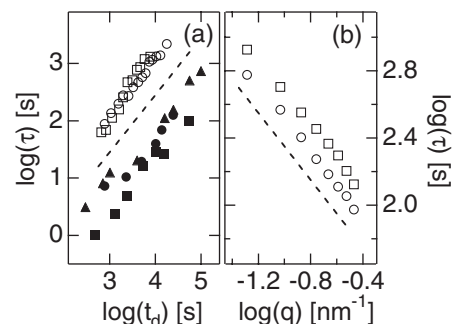


FIG. 2. (a) Characteristic relaxation times from XPCS (open symbols) at $q = 0.09 \text{ nm}^{-1}$ and from DWS (solid symbols) as a function of time since shearing. Results are shown for gels A (circles), B (boxes), and C (triangles). The dashed line displays the relation $\tau \sim t_d$. (b) Characteristic relaxation times for gels A (circles) and B (boxes) determined by XPCS at $t_d = 3200$ s as a function of wave vector. The dashed line shows the relation $\tau \sim q^{-1}$.

photomultiplier tube and CCD detection system, similar to that of Viasnoff *et al.* [31] along with a 400 mW Nd:YAG laser with wavelength $\lambda = 532$ nm. To initiate each measurement, the suspensions were extruded into glass cuvettes that were then sealed and placed in a temperature-controlled bath at 25 °C.

Figure 3 displays the intermediate scattering function determined by DWS for gel A at several recovery times. As observed with XPCS, $g_1(t)$ obtained with DWS evolves rapidly with time since shear and is described by a compressed exponential line shape $g_1(t) = \exp[-(t/\tau_D)^{\beta_D}]$. The solid lines in Fig. 3 are the results of fits to this form. Analysis of DWS measurements on the two suspensions studied with XPCS (gels A and B) and on a third suspension with $\phi = 0.28$ and $c_p/c_p^* = 0.15$ (gel C) finds that the compression exponent has a value $\beta_D = 1.3 \pm 0.07$, slightly smaller than the value obtained with XPCS. As shown in Fig. 2(a), the characteristic relaxation time τ_D obtained with DWS also scales linearly with t_d . The similar line shapes with XPCS and DWS and the similar scalings of relaxation time with t_d suggest that the two experiments probe the same motion. To make this connection quantitative, we analyze the DWS results to extract a characteristic velocity for ballistic motion and compare it with that obtained with XPCS. In DWS, the light is multiply scattered within the sample leading to a distribution of path lengths s and a corresponding intermediate scattering function [30]:

$$g_1(t) = \int P(s) \left[\exp\left(-\frac{1}{3}k_0^2 \langle \Delta r^2(t) \rangle\right) \right]^{s/l^*} ds, \quad (1)$$

where $P(s)$ is the path-length distribution, l^* is the transport mean free path, $\langle \Delta r^2(t) \rangle$ is the mean squared displacement of the scatterers, and $k_0 = 2\pi/\lambda$. For ballistic motion with velocity \vec{v} , $\langle \Delta r^2(t) \rangle = \vec{v}^2 t^2$. However, the existence of a distribution of velocities $G(\vec{v})$ [24] implies that the phase factor $\exp(-\frac{1}{3}k_0^2 \vec{v}^2 t^2)$ is averaged over this distribution. For the distribution implied by the XPCS line shape, asymptotically given by $G(\vec{v}) \sim |\vec{v}|^{-(\beta+1)}$, the integration

over velocities leads to

$$g_1(t) = \int P(s) \{ \exp[-(k_0 V_0 t)^\beta] \}^{s/l^*} ds. \quad (2)$$

As Eq. (2) indicates, the distribution of path lengths $P(s)$ in DWS broadens the intrinsic compressed exponential line shape. Calculations of such broadening for DWS in transmission geometry for simple diffusive dynamics show that it has a minor effect on the line shape [29], changing an exponential decay ($\beta = 1$) to a stretched exponential with $\beta_D \approx 0.84$ for typical values of L/l^* , where L is the sample thickness. Thus, our observation that β_D is slightly smaller than β measured with XPCS supports our assumption that the two exponents reflect the same distribution of velocities.

In principle, $P(s)$ can be determined from the experimental geometry, allowing more precise comparison of the line shapes. However, this determination requires knowledge of the cross section of the scattering elements, in this case particle clusters with unknown optical characteristics for which an evaluation of $P(s)$ is unfeasible. If we instead make the simple approximation of a single characteristic path length given by $s = L^2/l^*$, then Eq. (2) reduces to $g_1(t) = \exp[-(L/l^*)^2 (k_0 V_0 t)^\beta]$ [32]. Thus, we may relate the relaxation time measured with DWS to the characteristic velocity using $\tau_D = [k_0 V_0 (L/l^*)^{2/\beta}]^{-1}$. Using $(L/l^*) \approx 22$, as determined by comparing transmitted light intensity with that of samples of known l^* , we extract characteristic velocities from the DWS results shown in Fig. 4. Also shown are the characteristic velocities determined from the XPCS results through the relation $V_0 = 1/(\tau q)$. The values for V_0 obtained from the two techniques display remarkable overlap despite the approximations used to derive them.

This agreement between XPCS and DWS suggests a specific microscopic picture for these ballistic dynamics. While DWS is sensitive to subnanometer-scale motion, the scattering entities must be micron-scale to assure adequate scattering. The x-ray intensity, on the other hand, is domi-

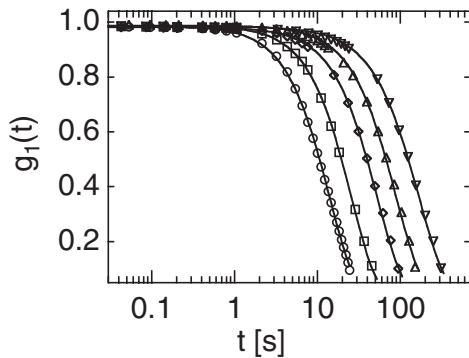


FIG. 3. DWS intermediate scattering function for gel A at recovery times $t_d = 2300$ (circles), 5000 (boxes), 10000 (diamonds), 14000 (triangles), and 24000 s (∇). The solid lines are the results of fits to a compressed exponential form.

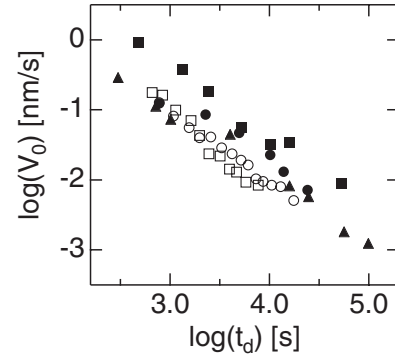


FIG. 4. Characteristic velocity for ballistic motion as a function of recovery time determined from XPCS (open symbols) and from DWS (solid symbols). Symbols refer to the same gels as in Fig. 2(a).

nated by correlations between nearest neighbor colloids. Hence, XPCS directly probes the motion of the individual colloids. The quantitative agreement between the motion detected by the techniques thus indicates the absence of internal dynamics among the colloids below the micron scale. Detailed analysis of SAXS measurements indicates that the colloids form dense clusters of size $\approx 10R$ [21]. The combined XPCS and DWS results can be understood by interpreting the dynamics as ballistic motion of these clusters in response to internal stress, with the structure of the clusters remaining arrested. Specifically, the shear restructures the jammed network of clusters in a way that creates mechanically weak regions and introduces internal stress. As weak regions fail, leading to local restructuring, the rest of the network strains as the stress in the network redistributes. The motion that we observe is this strain. A compressed exponential line shape with $\beta = 1.5$ is consistent with strain from dipole stress fields [24], indicating that the restructuring involves isolated, highly local events that further have a negligible effect on $I(q)$. With increasing t_d , the rate of events decreases, leading to a decrease in V_0 and concomitant increase in τ .

The identification of the dynamics of recovery with such elastic deformation calls into question its relationship to aging of glasses. The glass transition in supercooled liquids occurs at a temperature where the structural relaxation times exceed experimental times, and aging is observed below this temperature. Hence, following a quench $\tau > t_a$, where t_a is the aging time. In contrast, the particle-scale dynamics of the sheared depletion gels and other soft solids have $\tau \ll t_d$ at even the earliest t_d , precluding direct identification of the observed dynamics with the nonergodic degrees of freedom. Further, analysis of dielectric susceptibility studies of aging in supercooled liquids shows how it is a manifestation of the structural relaxations returning to equilibrium in an age dependent manner [6,7]. Thus, the characteristic relaxation time varies with age in a complicated way, and these canonical aging systems do not display $\tau \sim t_a$ scaling analogous to Fig. 2(a) and typically considered a hallmark of aging. Of course, the structural relaxations in nonergodic soft solids could similarly evolve. However, in correlation measurements such as XPCS and DWS, the translational ballistic motion of material due to stress relaxation masks possible slower dynamical equilibration. An experiment that could simultaneously characterize both types of dynamics would be most valuable. One approach might be to use direct optical tracking of jammed colloidal particles to decouple ballistic and diffusive dynamics. Another possibility might be to study jammed nanoparticle dynamics with XPCS in a heterodyning mode with a focused beam.

We thank V. Gopalakrishnan, S. Narayanan, and A. Sandy for their assistance. Funding was provided by the NSF (DMR-0134377). Use of the APS was supported by the DOE, Office of Basic Energy Sciences, under Contract No. W-31-109-Eng-38.

*Corresponding author.

Electronic address: jharden@science.uottawa.ca

†Corresponding author.

Electronic address: leheny@pha.jhu.edu

- [1] Y.-L. Chen and K. S. Schweizer, *J. Chem. Phys.* **120**, 7212 (2004).
- [2] K. N. Pham *et al.*, *Science* **296**, 104 (2002).
- [3] L. Fabbian *et al.*, *Phys. Rev. E* **59**, R1347 (1999).
- [4] See, for example, *Jamming and Rheology*, edited by A. J. Liu and S. R. Nagel (Taylor & Francis, London, 2001).
- [5] V. Trappe *et al.*, *Nature (London)* **411**, 772 (2001).
- [6] R. L. Leheny and S. R. Nagel, *Phys. Rev. B* **57**, 5154 (1998).
- [7] P. Lunkenheimer *et al.*, *Phys. Rev. Lett.* **95**, 055702 (2005).
- [8] M. Cloitre, R. Borrega, and L. Leibler, *Phys. Rev. Lett.* **85**, 4819 (2000).
- [9] V. Viasnoff, S. Jurine, and F. Lequeux, *Faraday Discuss.* **123**, 253 (2003).
- [10] C. Derec *et al.*, *Phys. Rev. E* **67**, 061403 (2003).
- [11] S. M. Fielding, P. Sollich, and M. E. Cates, *J. Rheol. (N.Y.)* **44**, 323 (2000).
- [12] C. Derec, A. Ajdari, and F. Lequeux, *Eur. Phys. J. E* **4**, 355 (2001).
- [13] L. Berthier, J.-L. Barrat, and J. Kurchan, *Phys. Rev. E* **61**, 5464 (2000).
- [14] J.-L. Barrat, *J. Phys. Condens. Matter* **15**, S1 (2003).
- [15] D. J. Lacks and M. J. Osborne, *Phys. Rev. Lett.* **93**, 255501 (2004).
- [16] M. L. Wallace and B. Joos, *Phys. Rev. Lett.* **96**, 025501 (2006).
- [17] B. A. Isner and D. J. Lacks, *Phys. Rev. Lett.* **96**, 025506 (2006).
- [18] W. C. K. Poon, *J. Phys. Condens. Matter* **14**, R859 (2002).
- [19] S. A. Shah *et al.*, *J. Chem. Phys.* **118**, 3350 (2003).
- [20] S. A. Shah *et al.*, *J. Phys. Condens. Matter* **15**, 4751 (2003).
- [21] S. Ramakrishnan *et al.* *Phys. Rev. E* **70**, 040401(R) (2004).
- [22] We model the extruded gel as a power-law fluid $\sigma \sim \dot{\gamma}^n$, with $n = 0.5$, in the laminar flow regime.
- [23] D. Lumma *et al.*, *Rev. Sci. Instrum.* **71**, 3274 (2000).
- [24] L. Cipelletti *et al.*, *Faraday Discuss.* **123**, 237 (2003).
- [25] L. Cipelletti *et al.*, *Phys. Rev. Lett.* **84**, 2275 (2000).
- [26] R. Bandyopadhyay *et al.*, *Phys. Rev. Lett.* **93**, 228302 (2004).
- [27] M. Bellour *et al.*, *Phys. Rev. E* **67**, 031405 (2003).
- [28] J.-P. Bouchaud and E. Pitard, *Eur. Phys. J. E* **6**, 231 (2001).
- [29] D. A. Weitz and D. J. Pine, in *Dynamic Light Scattering: The Method and Some Applications*, edited by W. Brown (Clarendon, Oxford, 1993).
- [30] F. Scheffold and P. Schurtenburger, *Soft Mater.* **1**, 139 (2003).
- [31] V. Viasnoff, F. Lequeux, and D. J. Pine, *Rev. Sci. Instrum.* **73**, 2336 (2002).
- [32] This approximation of a single scattering path cannot capture the broadening of $g_1(t)$ in multiple scattering that leads to $\beta_D < \beta$.